NASA Technical Memorandum 87239

Adhesion and Wear Resistance of Materials

Donald H. Buckley
Lewis Research Center
Cleveland, Ohio

Prepared for the
Hartstoffschichten zur Verschleißminderung
sponsored by the Max-Planck-Institute für Metallforschung
Bad Honnef, Federal Republic of Germany, May 5–7, 1986

NASA

ADHESION AND WEAR RESISTANCE OF MATERIALS

Donald H. Buckley
National Aeronautics and Space Administration
Lewis Research Center
Cleveland, Ohio 44135

SUMMARY

Recent studies, both analytical and experimental, into the nature of bonding at the interface between two solids in contact or a solid and deposited film have lent considerable insight into adhesive bonding. This has provided a better understanding of those properties important to the adhesive wear resistance of materials. Both analytical and experimental progress in the field are reviewed. For simple metal systems the adhesive bond forces are related to electronic wave function overlap where electronic structure and total energy are computed as a function of separation between the surfaces. With metals in contact with nonmetals such as oxide ceramics and diamond, molecular-orbital energy, and density of states, respectively can provide insight into adhesion and wear of the solid state contacts. Experimental results are presented which correlate adhesive forces measured between solids and the electronic surface structures. Orientation, surface reconstruction, surface segregation, adsorption are all shown to influence adhesive interfacial strength. Examples are presented for various classes of materials comprising the interface. The interrelationship between adhesion and the wear of the various materials as well as the life of coatings applied to substrates are discussed. Metallic systems addressed include simple metals and alloys and these materials in contact with themselves, both oxide and nonoxide ceramics, diamond, polymers, and inorganic coating compounds, such as diamond-like carbon. The role and mechanism of interfacial foreign species on adhesive bonding will also be presented.

E-2914

INTRODUCTION

When two solids are placed into solid-state contact in the atomically clean state strong adhesive bonds develop across the interface for most material pairs (ref. 1). In the case of two metals in contact electron wave functions from the two metals can overlap. This leads to large electron-exchange interactions. Charge transfer occurs when the metals are not identical. The total binding energy varies rapidly with spacing between the surfaces and large variations in electron density distribution occur in the interface (ref. 2).

With metals in solid-state contact with nonmetals chemical bonds can form at the interface and account for the strong adhesive interactions observed. From simple elementary molecular-orbital theory a bond is formed by partially occupied orbitals of similar energy. For example, with metals contacting diamond a bond forms between the Fermi level metal electrons and the empty gap states in diamond (ref. 3). Metals contacting ceramics such as sapphire bonding occurs via manifolds of spatially localized occupied metal (d)-oxygen (p) bonding molecular orbitals (ref. 4). When polymers contact metals the bonds formed can be of sufficient energy intensity so as to result in the formation of interfacial inorganic compounds (ref. 5).

The strong interfacial adhesive bonds formed between two solids contributes to one of the most severe forms of wear, namely adhesive wear. Material is also lost from solid surfaces by other mechanisms as well. These include abrasion, corrosion, cavitation, fretting, and erosion. While these latter forms of wear do not involve adhesion directly, it is to a degree present in some of these other wear forms (ref. 6).

The application of hard face coatings to surfaces to improve wear resistance requires strong adhesion of coatings to the substrate with poor adhesion between contacting members to minimize adhesive wear. Adhesion is therefore an important consideration in thin film coating technology particularly for tribological applications.

The objective of this paper is to review the fundamental nature of adhesive bonding between solids, the nature of that bonding to wear mechanisms and its importance to hard face coating technology. Both theory and experimental observations will be considered. Material classes to be discussed will include metals, ceramics, polymers, and hard face coatings of diamond-like carbon and refractory metal carbide films.

RESULTS AND DISCUSSION

Atomic Nature of the Adhesion Process

Metal to metal. - In considering the nature of adhesion between two solid surfaces the simplest approach theoretically is to consider the bimetallic interface. This then logically involves the solving of the Kohn-Sham equations self-consistently for a bi-jellium model. A bi-jellium model is shown in figure 1 for the Al(111)-Mg(0001) interface. There are two jellia uniform density backgrounds. These are separated by a distance α. This nearly free-electron model is only valid for simple metals. By charge neutrality, $\alpha = 0.0$ when the distance between Al and Mg atomic planes is $d_{Al} + d_{Mg}/2$ where d_{Al} and d_{Mg} are distance between planes of atoms in the two metals.

Using the model of figure 1 together with Kohn-Sham equations for the electron density it is possible to transform a many electron problems into an effective one electron model which is valid for a computation of the total interfacial binding energy. This has been effectively done (ref. 7). A further extension of the theory has been the inclusion of crystal structure for the pair of metals with first order perturbation theory (ref. 8).

As a result of the foregoing the adhesive interaction energy, E_{ad}, between two metals separated by the distance is calculable in accordance with the simple equation:

$$E_{ad} = [E(a) - E(\infty)]/2A$$

where A is the cross-sectional area.

The self-consistent electron density distributions and accordingly the adhesive interfacial bond forces are very sensitive to small changes in interfacial separation. This effect is demonstrated in the data of figure 2. In figure 2 the Al-Mg interface (Al is on the left) is presented for three separations, a = 0.0, 0.16, and 1.6 nm (0, 3, and 30 au).

Ignoring interfacial defects and lattice distortions one then can calculate total interfacial adhesive energies. If this is done for a series of simple bimetallic couples it is established that strong adhesive forces exist for a surface separation distance of about 0.2 nm. This is roughly equivalent to a bulk interplanar spacing.

It is anticipated that some metal couples have shorter screening lengths than others, that is the metals would screen the disturbances caused by creating the surface over a shorter distance. For identical metal contacts the separation is scaled by the Thomas-Fermi screening length $\lambda = (9\pi/4)^{1/3} V_s^{1/2}/3$ au where the bulk electron density is is $n_+ = 3/4\pi r_s^3$. With bimetallic contacts a length screening approach to both metals must be considered. In such a case scaling is done by an arithmetic average. The energy values from such calculations can also be scaled by using equilibrium separation values, $E \equiv E_{ad}(a_m)$ where a_m is the equilibrium separation.

Figure 3 presents the scaled adhesive energy values for the bimetallic contacts as a function of separation. All of the points lie very close to a universal curve derived from the universal adhesion energy function $E_{ad}*(a*)$ coming from the relationship:

$$E_{ad}(a) = \Delta E\, E_{ad}*(a*)$$

where $a* = 2/(a-a_m)/(\lambda_1 + \lambda_2)$

The universal nature of the curve is very remarkable since the bulk metallic densities in the various metals varies by a factor of eight.

Once having established the universal nature of bimetallic adhesion one can examine the individual energies which constitute the total energy. If we continue with the same contact pair addressed in figure 1 namely the Al(111)-Mg(0001) contact and examine the self consistent energy components of the binding energy, at large separations (>0.2 nm) the kinetic energy component is negative with respect to infinite separation of the metals. It is this kinetic energy which initiates the formation of a bond presumably due to the smoothing out of the electron wave functions in the bonding region. The electrostatic energy is positive at these same large separations but changes sign at smaller separations. It is worthwhile to note that the dominant attractive energy component is the exchange-correlation energy while the principle repulsive term at small separations in the kinetic energy. Figure 4 presents the binding energy considerations for the bimetallic interface. A similar behavior exists for identical metals (ref. 9).

Metal to diamond. - The metal to diamond interface and the adhesive forces that develop between two such solids are of considerable interest. Diamond is widely used in industrial metal removal processes and diamond-like plasma physics deposited films have been applied to metal substrates. In both instances the nature of interfacial bonding of the metal to diamond is important.

Recent studies using surface analytical techniques such as electron energy loss spectroscopy (EELS) have revealed the surface of diamond undergoes a transformation in its electronic structure when heated above 900 °C. A normal polished diamond surface has no electronic states in the band gap. When the surface is annealed by heating above 900 °C diamond has both occupied and

unoccupied states in the band gap. The annealed surface also exhibits some electrical conductivity.

Static friction studies for metals in contact with the diamond surface reveal that this transformation has a strong effect on interfacial bonding. Bonding is weak for the diamond in the polished state with static friction being low and strong for diamond in the annealed state resulting in high static friction. This is accordingly accompanied by transfer of metal to the diamond surface and metallic wear. These effects can be seen in the static friction data of figure 5 for copper in contact with the (111) surface of diamond at various temperatures.

In figure 5 annealing to 900 °C removes adsorbed hydrogen and causes a increase in static friction with adherence and transfer of metal to the diamond surface. Exposure to excited hydrogen at 900 °C causes an immediate reduction in static friction and metal transfer (wear) is arrested.

The foregoing observations have been made for both the (111) and (110) surfaces of diamond. The change in interfacial bond strength accounting for a change in adhesion, static friction, and metal transfer (wear) can be explained in terms of elementary concepts of molecular orbital theory.

From elementary molecular-orbital theory of chemical bond formation a bond is formed by partially occupied orbitals of similar energy. These bonds are indicated schematically in figure 6 for diamond. On the right side of figure 6 the orbitals that constitute the valance band are fully occupied while the orbitals that constitute the conduction band are empty. Thus, for the diamond surface with a large band gap between the valence and conductive band and without gap states, the Fermi level electrons of the metal in figure 6 must interact with the (empty) conduction band orbitals in the diamond to form a chemical bond. The energy difference between the bottom of the conduction band and the Fermi level is too large to allow a bond to form and this then accounts for weak adhesion at the interface.

Once the diamond surface has been annealed the unoccupied states in the band gap lie much closer in energy to the Fermi level and this smaller energy difference allows for the formation of a bond by the Fermi level metal electrons and the empty gap states. Such a bond increases interfacial strength and the diamond surface is conducting figure 6 (left side). The bond increases interfacial strength, leads to higher friction, and greater metal transfer. This chemical bonding explanation requires the energy of the unoccupied surface states to be in the band gap of the crystalline ground state.

A logical question imminating from the bond formation between diamond and a metal is does bond strength vary with the metal? Examination of various transition and rare earth metals in contact with diamond reveal the effect of d-bond character on interfacial bond strength to diamond, adhesion, friction force, and material transfer (wear). This effect can be seen by way of example in the friction data of figure 7.

Examination of figure 7 reveals that the metals with the greatest d valence bond saturation, i.e., platinum metals exhibit the weakest interfacial bonding, as evidenced by friction coefficient, while those metals with the greatest degree of unsaturation, titanium, and the rare earth metal yttrium exhibit the greatest.

Metal-ceramic. - When metals contact oxide ceramics such as aluminum oxide strong adhesive bonds can develop just as for metals in contact with metals and the diamond structure. If, for example, atomically clean copper is placed in solid-state contact with the basal (0001) plane of sapphire the adhesive bonds formed are sufficiently strong so as to cause fracture in the sapphire along basal cleavage planes subsurface. Evidence for this can be seen in the photomicrographic insert of figure 8.

In figure 8 friction coefficient is presented for two specimen configurations, a copper hemisphere on a sapphire flat and a sapphire hemisphere on a copper flat. With both configurations the interfacial adhesive bond forces are the same and are reflected in the friction coefficient of 0.2 for the copper hemisphere on the sapphire flat. The difference between the two friction values is related to the plastic deformation and plowing of the copper by the sapphire hemisphere.

Copper forms stable oxides and it can reasonably be assumed that it is the copper to oxygen ion bonding at the basal planar surface that accounts for the interfacial adhesion. If this is true, then, relatively weak interfacial bonds should form for sapphire in contact with silver or gold which do not form stable metal oxides. Repeating the experiment of figure 8 for the metal hemisphere on the sapphire flat with the substitution of silver and gold for copper produces the results of figure 9.

The friction coefficient in figure 9 for both silver and gold are one-half the value seen in figure 8 for copper. Further, examination of the wear surfaces of sapphire reveal a complete absence of fracture cracks in figure 9. The obvious weak region was not in the sapphire but at the interface since there was an absence of fracture cracks in the sapphire and no evidence of metal transfer to the sapphire to support a conclusion that the weakest region was in the metal. The friction coefficients of figure 9 reflect extremely weak interfacial bonding as these values would typically be obtained where the solid surfaces were separated by a boundary lubricating film.

Additional experiments to those of figures 8 and 9 with other metals confirmed a chemical bond forms between the metal and the oxygen ions of the sapphire surface. The shear strength of the metal-sapphire interface were correlated with the chemical energy of formation of the metal oxide (ref. 10). This bonding process, which results in wear to the sapphire can be explained in a more fundamental manner by examining molecular-orbital energies for clusters in bulk sapphire and the metal to sapphire interface.

Figures 10 and 11 explain the interfacial bonding mechanism in greater detail. Bonding at the interface occurs between the metal d orbitals and the normally nonbonding p orbitals of the oxygen ions at the surface of the sapphire crystal. These would be the nonbonding p orbitals at the top of the valence band. An examination of figure 10 reveals that the d orbital energies of the specific metal atoms are in close proximity to the sapphire valence band. The relative position of the metals to the top of the sapphire valence band changes systematically through the series, Fe, Ni, Cu, and Ag.

The metal to sapphire contact interaction produces at the interface manifolds of spatially localized occupied metal (d) and oxygen (p) bonding molecular orbitals of energies near the bottom of the sapphire valence band and metal (d) with oxygen (p) antibonding molecular orbitals of energies near the top of

the sapphire valence band. This is exemplified for iron in contact with sapphire by bonding and antibonding orbital wave-function contour maps of figures 11(a) and (b), respectively.

With iron and nickel the antibonding orbitals are only partially occupied and are located well above the valence band within the band gap as indicated in figure 10. The antibonding Fe(d) and O(p) orbital mapped in figure 11(b) is unoccupied. Conversely the silver antibonding orbitals are fully occupied and are located close to the top of the valence band.

There is an ionic component associated with metal to oxygen charge transfer at the metal to sapphire interface. This is in addition to the covalent and antibonding interactions. These results indicate that a chemical bond is in fact established between metal atoms and the oxygen anions on the sapphire surface and that the ionic component of bonding is proportional to the metal (d) and oxygen (p) orbital electronegativity difference.

With respect to relative bond strength the occupation of antibonding molecular orbitals tends to cancel the effects of occupied bonding orbitals and this reduces the net chemical bond strength when compared to the situation where only bonding orbitals are occupied. The increase in occupancy of the metal-sapphire antibonding orbitals through the series Fe, Ni, Cu, and Ag therefore should tend to lower the net metal to sapphire chemical bond strength and this correlates with the significant reduction in metal to sapphire contact strength and accordingly the adhesion to sapphire of these series of metals.

The decrease in the friction coefficient from 0.2 for copper to 0.1 for gold or silver can be explained qualitatively by the combined effects of increasing antibonding orbital occupancy and decreasing the metal to oxygen charge transfer. The small friction coefficients and interfacial bond forces measured for gold and silver, 0.1 is consistent with the fully occupied antibonding orbitals of figure 10 cancelling the covalent contributions of the bonding orbitals, leaving only small residual ionic and van der Waals contributions.

In general the presence of adsorbates or other contaminants on a solid surface destroys the strong binding energies discussed for metals in contact with metals, diamond, and oxide ceramics. This was observed, for example, in figure 5 when the diamond surface was exposed to excited hydrogen. There are, however, exceptions to this general observation. Oxygen can, for example, in the case of metal to ceramic oxide contacts act as an adhesive promoting the strength of the interfacial chemical bond. Evidence for this can be found in the data of figure 12.

Friction coefficients reflecting interfacial bond strengths are greater for metals in contact with the oxide ceramic, nickel-zinc ferrite when the clean surfaces have been exposed to 1000 L of oxygen. The exact role of the oxygen in increasing bond strength is not known but is believe to be related to the formation of a spinel type structure at the interface.

Wear Mechanisms

Adhesive wear. - As already mentioned adhesive wear is one of the most severe types of wear and occurs when interfacial solid-state bonding takes

place. In general the interfacial bond strength is greater than the bond strength in the cohesively weaker of the two materials comprising the interface. One notable exception was that already discussed for the noble metals silver and gold in contact with the aluminum oxide surface.

An example of the general material pair behavior is seen in the field ion micrograph of figure 13. This figure resulted from conducting "in situ" adhesion experiments in the field ion microscope with gold contacting a tungsten ion tip. Upon separation of the solids gold atoms remain adhered to the tungsten surface. The gold atoms lie in clusters of three about each tungsten atom as indicated in figure 13. The clustering reflects the formation of the interfacial compound WAu_3. This particular compound does not exist in the bulk and is truly the product of interfacial adhesive interactions.

For the metal pairs of figure 13 and metal pairs in general the adhesive transfer and accordingly wear of one component is arrested by the presence of adsorbed oxygen or chemically active species.

With alloys many properties effect adhesion, transfer, and wear. These include surface segregation of alloying elements at the interface, crystal structure, crystal orientation, texturing, stacking faults, order-disorder reactions, and environmental chemical interactions. The effectiveness of materials to act as lubricants for alloys is determined in many practical test devices by the ability of the materials to resist adhesive wear.

Abrasive wear. - There are two forms of abrasive wear, namely two-body and three-body mechanisms. In the two-body mechanism material is removed from one of two surfaces because of basic material property differences between the solids. Further, consideration to the single solid undergoing abrasive wear indicates that material loss due to wear is effected by fundamental material behavior.

In figure 14 iron binary alloys were abraded by silicon carbide. The data of figure 14 indicate a relationship between solute to iron atomic radius ratio with average decreasing groove height produced on the alloy surface by the abrading silicon carbide.

When the atomic radius of the solute atom is either larger or smaller than the solvent atom, iron sufficient lattice strain is produced so as to alter the resistance of the alloy to abrasion.

Corrosive wear. - Corrosive wear occurs when the environment interacts with mechanically interacting surfaces resulting in an increase in wear. It is undesirable when uncontrolled but needed in the effective utilization of anti-wear additives, which represents controlled corrosion.

Corrosive attack and its effect on the wear process can be seen in the data of figure 15 for an iron surface in water and various concentrations of sodium hydroxide. The surface profiles of figure 15 reflect the wear occurring to the iron surface. Static friction coefficients are also presented in figure 15. The data indicate that corrosive wear is not a simple function of the concentration as the greatest amount of wear, as indicated by the surface profiles, occurs with the two of the four weakest concentrations of sodium hydroxide.

While in figure 15 there appears to be some relationship between friction and wear there need not be any interdependence. Very frequently the surface films that form as a result corrosive attack can provide extremely low friction while the wear rates are extremely high. This is generally observed to be the case for halogen containing environments where metallic components are undergoing corrosive wear.

Cavitation. - Another form of wear which occurs in fluid systems such as hydraulics, pumps, valves, ships' propellers, bearings, gears, and seals involves the impingement of fluids on solid surfaces, gas bubble formation, and bubble collapse on the surfaces. The collapse of the impinging bubbles results in energy transfer and material loss from the solid surface. The energy is sufficient to produce notable losses from the solid surface.

Fundamental cavitation studies indicate that this form of wear is surface orientation dependent in its morphology as an example of one property that can be related to wear by cavitation. There are many others and the reader is referred to the literature for these (ref. 11).

The orientation dependency effect can be seen in the data of figure 16 for brass single crystals. The cavitating fluid was a mineral oil with two orientations being examined, the (001) and (110) faces of the brass. A pit very analogous to an etch pit formed in the (001) face with the walls of the pit lying along the <110> directions. The corners of the pits are rounded (fig. 16(a)). Cavitation of the (110) face results in an elongated crater running along the <110> direction as indicated in (fig. 16(b)). Pit formation (wear) occurs more rapidly at grain boundaries and grain boundary intercepts than over the individual grains. Likewise, rapid pit formation occurs around precipitates. All of the foregoing indicates the surface energetics dependency of cavitation behavior, a wear process.

Fretting. - A very severe form of wear experienced in a host of mechanical devices is that of fretting. This form of wear has actually two other wear mechanisms involved in it. These are adhesion and corrosion. It occurs in devices where there are small amplitudes of reciprocating motion between two solids. Initially protective surface films are removed by the reciprocal rubbing process. This exposes nascent materials at the interface and adhesive wear particles are generated. These are generally very small in size, in a highly strained state and therefore energetic on their surfaces. This leads to reaction with environmental constituents. In air for metals it results in the formation of surface oxides.

Because of the highly reactive state of the wear particles surfaces excessive quantities of reaction products are formed. For example, in the case of ferrous-base metallic systems it results in rapid formation of ferric oxide. This is an abrasive material and it precipitates yet another form of wear, namely, that of abrasion. Where the oxides have lower shear strengths than the substrates upon which they find themselves the latter form of wear generally will not occur. Coatings have proven very effective in arresting this form of wear.

Erosive wear. - From what has been said thus far, it must be apparent that surfaces are extremely important to the wear behavior of materials. Further, from the discussion on the cavitating process surface energetics are seen to

play an important role. The effect of surface energy are also seen in the erosion of solids surfaces.

Erosion occurs to a solid surface when that surface is impacted at relatively high energies by particulate matter. Many parameters influence this form of wear. These include angle of incidence of the incoming particles to the surface, velocity of the particle, its size, shape, and composition.

In fundamental studies of erosive wear the goal is to correlate erosive wear with material properties of the solid surface being eroded. One such property is surface energy. There appears to be a relationship between the erosive wear of elemental metals and their surface energies. The correlation can be seen in the data of figure 17. In general the higher surface energy metals have the lower wear. It must be remembered, however, that the metals have other properties which could equally easily be correlated with erosive wear, for example, cohesive binding energy. But then cohesive binding energy in the bulk is related to the surface energy.

Fatigue. - A very common form of wear found in such mechanical components as rolling element bearings is fatigue. This form of wear occurs when a surface is subjected to repeated stress cycles and after a finite number of cycles cracks initiate either surface or subsurface. The initially developed crack will grow until material is lost from the surface of the solid as a free particle. Defects as well as foreign substances are sources either within the material or at the surface that can serve as crack initiators.

Coatings

The application of coatings to tribological surfaces is to reduce adhesion, friction, and wear between contacting solids. In some instances the coatings have as their primary objective the reduction of wear, for example, in the use of hard face surface films. Frequently they are applied for lubrication where the basic objective is to reduce adhesion, friction, and wear.

Table I presents some typical materials used as coatings both as hard coats for wear resistant applications and as low shear strength lubricating films. The nitrides and carbides of titanium and the sulfide of molybdenum are the most commonly used coating materials for hard wear resistant films and low shear strength lubricating films, respectively. These films are applied to substrates by a host of different techniques. Plasma physics techniques, ion plating, sputtering etc. are very popular because of the abilities of controlling film thickness, morphology, density, chemistry, and interfacial adhesion. These films all, when properly applied, reduce wear to mechanical components.

Recently considerable interest has been shown in carbon films deposited from a plasma of hydrocarbons. These films can have near diamond-like properties. Such hard films it is believed will afford good wear resistance when applied to mechanical component substrates. Experimental tribological studies on these films indicate that they do indeed increase the resistance of surfaces to wear.

Experiments conducted in the authors' Laboratory with diamond-like carbon films indicate that they do in fact offer promise as wear resistant coatings. Ion beam deposited films were applied to a silicon (111) single crystal substrate. The silicon wafer was masked so that a coating was deposited on only one half of the wafer. Friction and wear experiments were then conducted on the wafer. The results obtained are presented in figures 18 and 19.

In figure 18 the coefficient of friction is plotted as a function of sliding time. The data indicates that the friction coefficient of the film is considerably less than it is for the silicon substrate. Further, the width of the wear track is reduced significantly as indicated in the photomicrograph of figure 19. There is an abrupt reduction in the width of the wear track when sliding is no longer on the silicon but rather on the film.

When plasma physics techniques are used to deposit protective hard face wear resistant films the plasma conditions can have a pronounced effect on wear behavior. This is demonstrated with the data of figure 20 where a molybdenum carbide film was deposited on a steel disk (440-C).

The data of figure 20 indicate that with zero substrate voltage bias friction was high and there was noticeably preceptable wear to the coating as indicated in the surface profile insert. When the bias was increased to 300 V the coefficient of friction decreased appreciably and no detectable wear to the coating was observed as indicated in the wear profile insert of figure 20. Thus, optimization of sputtering parameters must be considered if optimum tribological characteristics are to be achieved.

Not only are the parameters in the plasma deposition of coatings important but also the substrate chemistry. Studies with titanium diboride deposited on a 440-C steel indicate that oxidation of the substrate, while not markedly effecting wear does have an effect on friction coefficient as indicated in the data of figure 21. Note in figure 21 the three-fold reduction in friction coefficient for the coating deposited on the oxidized substrate over that observed for the coating on the etched surface.

CONCLUDING REMARKS

Strong bonds form between two solids whose surfaces are in the atomically clean state. When two metals are brought into close contact their electron wave functions overlap. This leads to large electron exchange interactions and when the metals are not identical to charge transfer. The interfacial energies vary markedly with spacing and rapid variation is also found in electron density distributions at the interface.

With metals contacting nonmetals such as oxide ceramics the use of simple molecular orbital theory can explain the interfacial adhesion observed experimentally. It demonstrates that metal to the oxygen of oxide ceramic bonding occurs and bonding energy is a function of the antibonding molecular orbitals. Similarly the strong bonds that form between metals and a clean diamond surface can be explained with elementary molecular-orbital theory of chemical bond formation. It explains interfacial bond strength, adhesive transfer of metal to the diamond surface and adhesive wear.

There are a host of wear mechanisms that account for the loss of material from the surfaces of solids. These include adhesive, abrasive, corrosion, cavitation, fretting, erosion, and fatigue wear. Adhesive wear strongly depends upon interfacial bonding between the solids and elements of it are seen in other wear forms such as fretting. There are fundamental material properties that can be related directly to wear observed by the various mechanisms.

With the deposition of hard face coatings the use of plasma physics techniques are currently commonly in use for tribological applications. Plasma parameters are important to the wear properties of the deposited films. Further, substrate conditions, for example, oxidation state have a direct effect on such properties, as the friction behavior of the coatings.

REFERENCES

1. D.H. Buckley, Surface Effects in Adhesion, Friction, Wear and Lubrication, (Elsevier, New York 1981).

2. J. Ferrante, J.R. Smith and J.H. Rose, Phys. Rev. Lett., 50, 1385 (1983). J. Ferrante and J.R. Smith, Phys. Rev. B, 31, 3427 (1985).

3. S.V. Pepper, J. Vac. Sci. Technol., 20, 643 (1982).

4. K.H. Johnson and S.V. Pepper, J. Appl. Phys., 53, 6634 (1982).

5. D.R. Wheeler, NASA TP-1728, (1980); D.H. Buckley and W.A. Brainard, in Advances in Polymer Friction and Wear, Polymer Sci. and Tech., Vol. 5A, edited by L.H. Lee, (Plenum Press, New York, (1974)).

6. D.H. Buckley, J. of Microscopy, 135, 119 (1984).

7. J.H. Rose, J. Ferrante and J.R. Smith, Phys. Rev. Lett, 47, 675 (1981).

8. J.R. Smith and J. Ferrante, in Surfaces and Disorders, Materials Science Forum, Vol. 4, edited by J.W. Halley (Trans. Tech. Publications, Aedermannsdorf, Switzerland, 1985). p. 21.

9. J. Ferrante and J.R. Smith, Phys. Rev. B, 19, 3911 (1979).

10. S.V. Pepper, J. of Appl. Phys., 47, 801 (1976).

11. F.G. Hammitt, Cavitation and Multiphase Flow Phenomenon, (McGraw Hill, New York, 1980).

TABLE I. - PROPERTIES OF WEAR RESISTANT COATINGS

(a) Hard-face materials

Material ↓ / Property →	Crystal structure	Lattice parameter (__)	Vac stability	Air stability	Hardness, kg/mm^2	Mc
TiC	FCC(NaCl)	a = 4.33	3140 °C	450 °C	2400	0.21
TiN	FCC(NaCl)	a = 4.24	2950	537	1770	.18
Ti_2N	Tetragonal	a = 4.41,c = 8.80	-------	------	----	----
HfN	FCC(NaCl)	a = 4 52	3387 °C	530	----	.15
HfC	FCC(B_1)	a = 4.64	3830	------	2600	----
SiC	----------	----------	*2300 °C*	*800*	----	*20*
SiC-α	Hexagonal	a = 3 07,c = 15 08	-------	------	2917	----
SiC-β	----------	a = b = c = 4 35	-------	------	----	----
Si_3N_4-α	Hexagonal	a = 7.75,c = 5.62	1871 °C	1000	1950	.24
Si_3N_4-β	Hexagonal	a = 7.61,c = 2.71	-------	------	----	----

(b) Soft lubricating films

Material ↓ / Property →	Crystal structure	Molecular weight	Vac. stability	Air stability	Mc
MoS_2	Hexagonal	160 07	900 °C	350 °C	[b]0.05
$MoSc_2$	↓	253.86	750	400	.05
WS_2	↓	247.98	850	400	.05
WSc_2	↓	341.78	700	350	.05
Graphite	↓	12.01	3700	350	.20
PTFE	---------	$3.5x10^6$	327	300	.10
HDPE[a]	---------	$4.0x10^6$	110	------	.21

[a]High density polyethylene.
[b]Vacuum

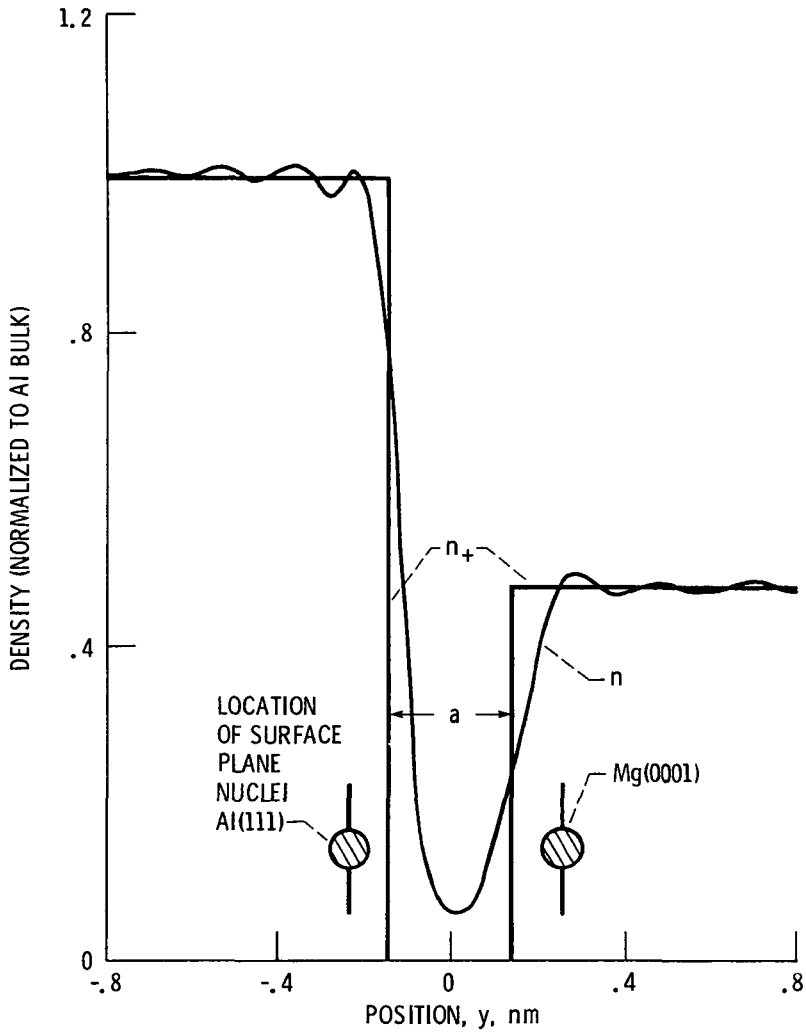

Figure 1. - Electron number density n and jellium ion charge density n_+ for an Al-Mg contact. When a = 0.0, the distance between Mg and Al atomic planes is $(d_{Al} + d_{Mg})/2$, where d_{Al} and d_{Mg} are the respective bulk interplanar spacings.

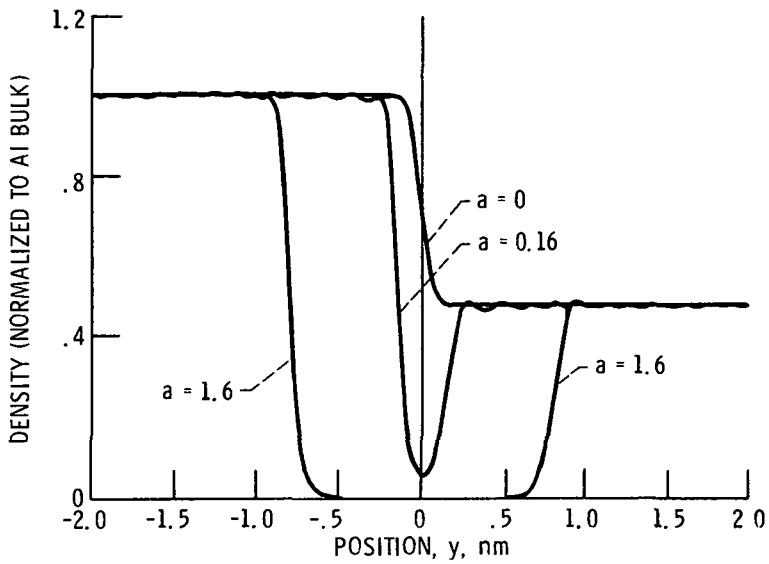

Figure 2. - Electron density versus position for an Al-Mg contact (Al is on the left), for separations of 0, 0.16, and 1.6 nm.

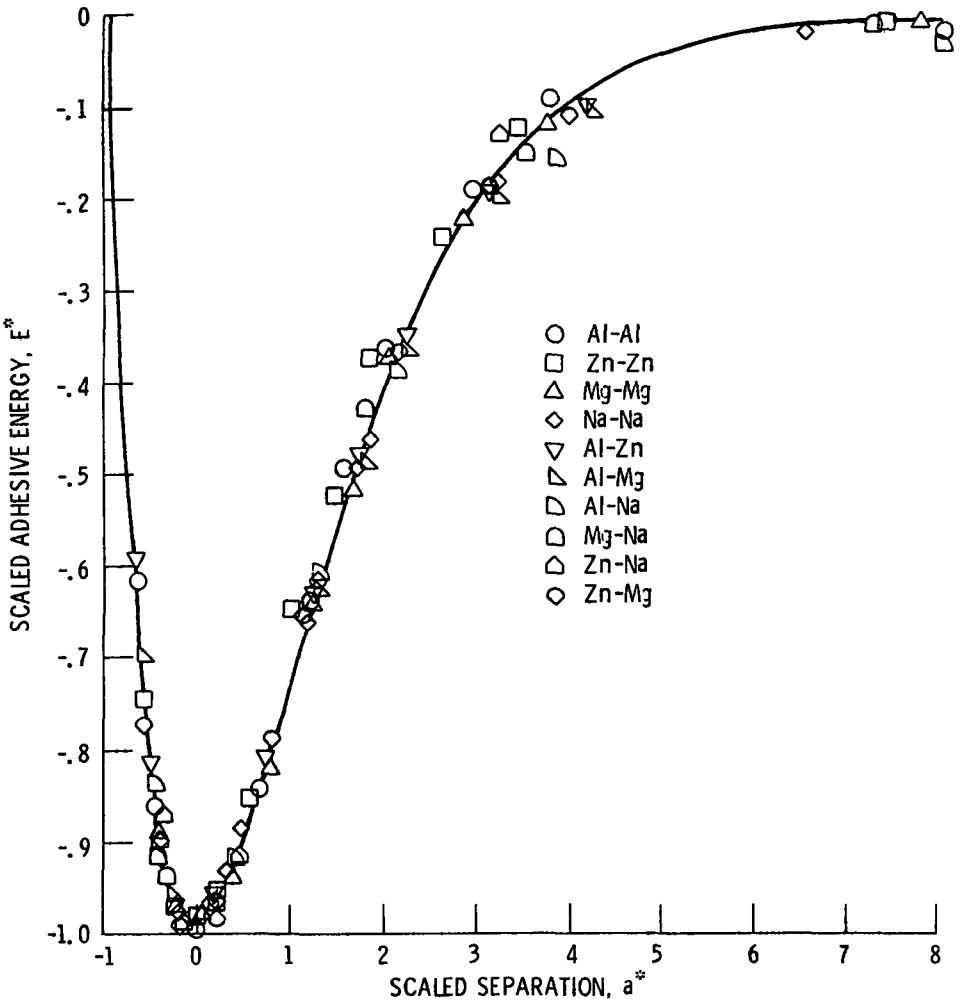

Figure 3. - Adhesive energy results scaled as described in the text.

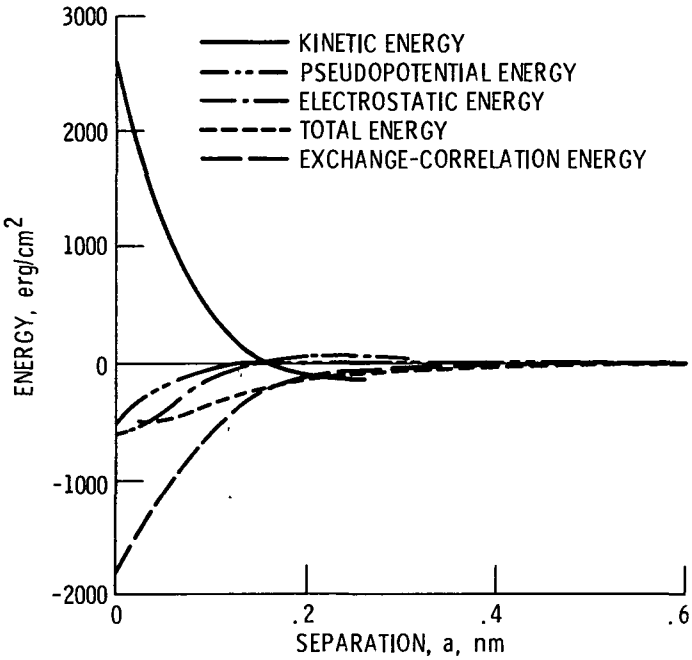

Figure 4. - Self-consistent energy components of the binding energy for an Al(111)-Mg(0001) contact.

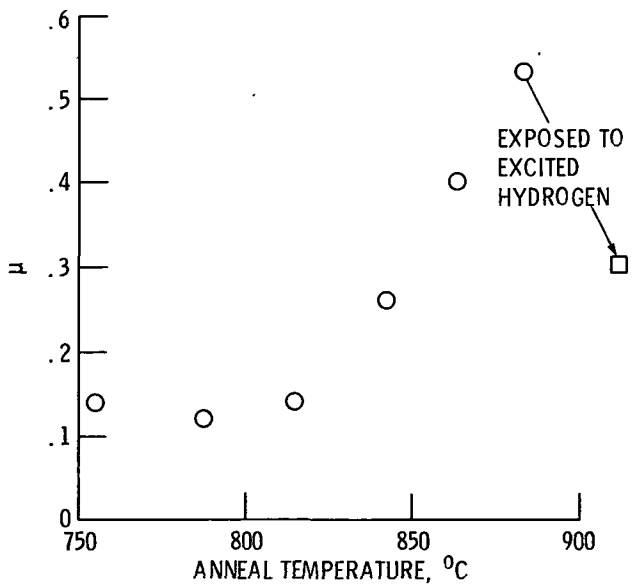

Figure 5. - Static friction coefficient for copper in contact with a diamond (111) surface at various temperatures. Removal of adsorbed hydrogen results in a friction increase and exposure to excited hydrogen at 900 °C results in an increase.

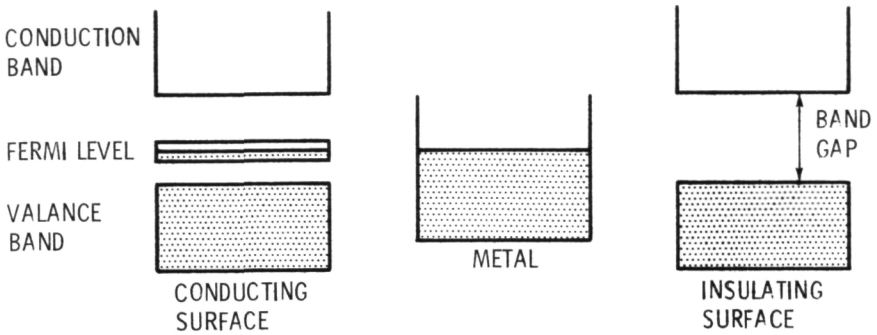

Figure 6. - Band picture of metal/diamond bond.

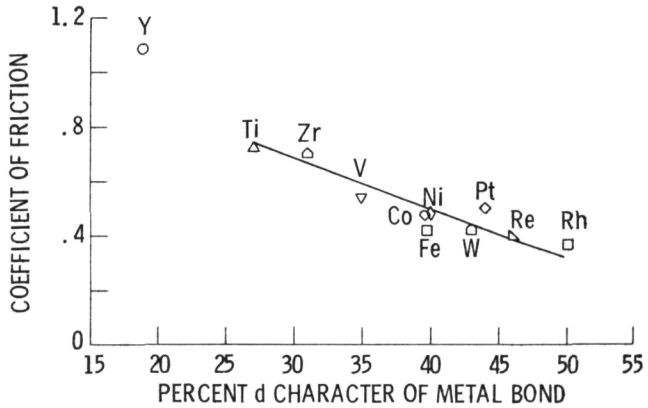

Figure 7. - Coefficient of friction as function of percent of metal d bond character for single-crystal diamond {111} surface in sliding contact with transition metals in vacuum. Sliding direction, $\langle 1\bar{1}0 \rangle$; sliding velocity, 3×10^{-3} m/min; load, 0.05 to 0.3 N; room temperature; vacuum pressure, 10^{-8} Pa.

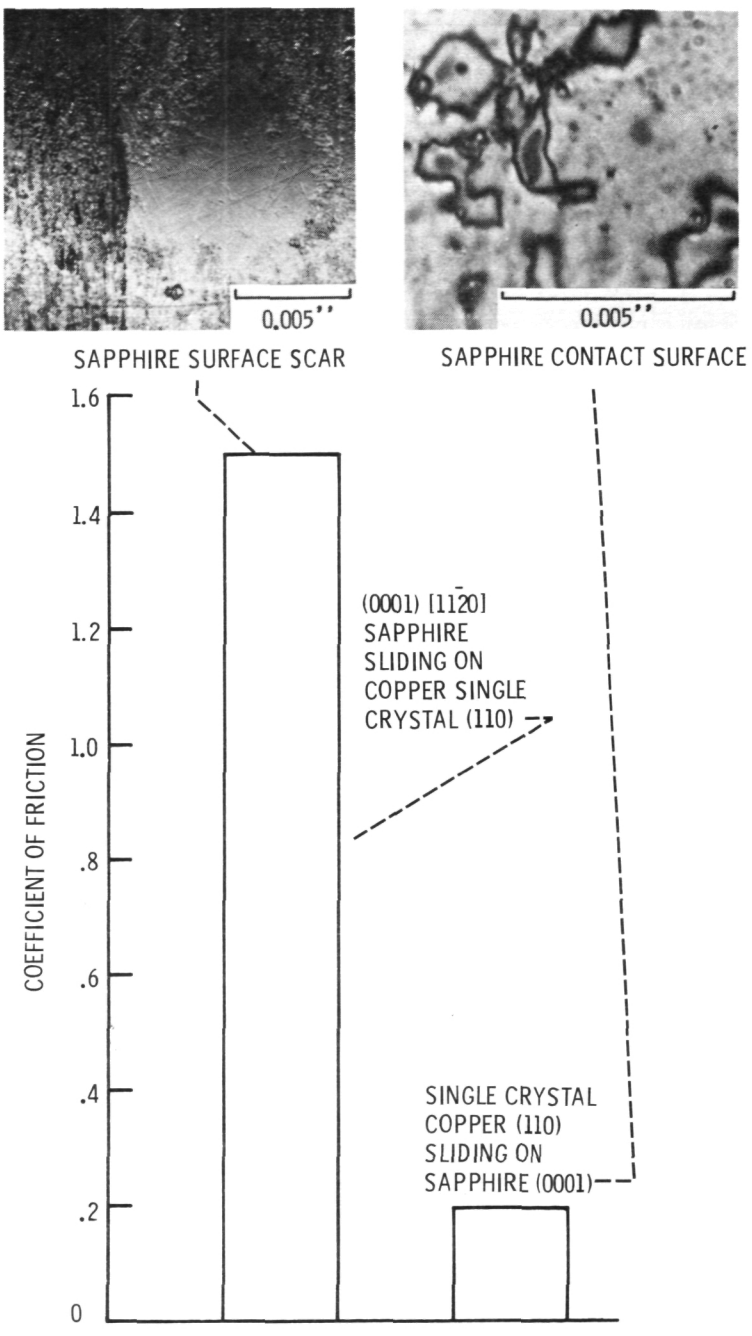

Figure 8. - Coefficient of friction for copper in sliding contact with sapphire in vacuum (30 nPa). Load, 0.5 N, sliding velocity, 0.013 centimeter per second.

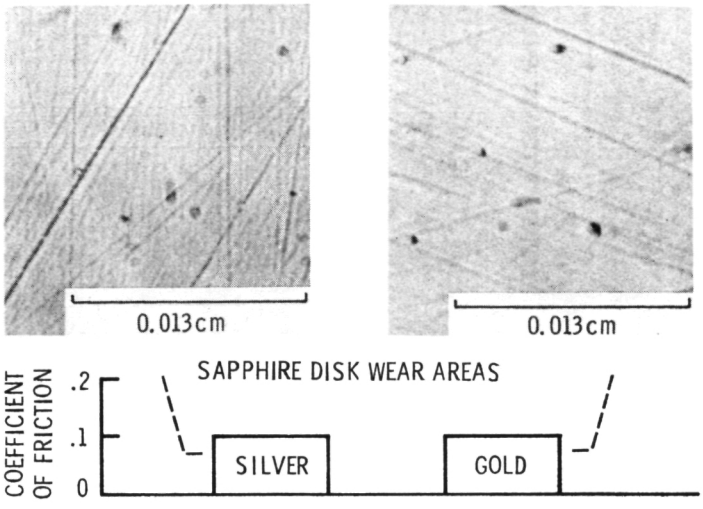

Figure 9. - Coefficient of friction for gold and silver riders sliding on sapphire in vacuum (30 nPa). Sliding velocity, 0.013 centimeter per second; ambient temperature, 298^{0} K; duration, 1 hour.

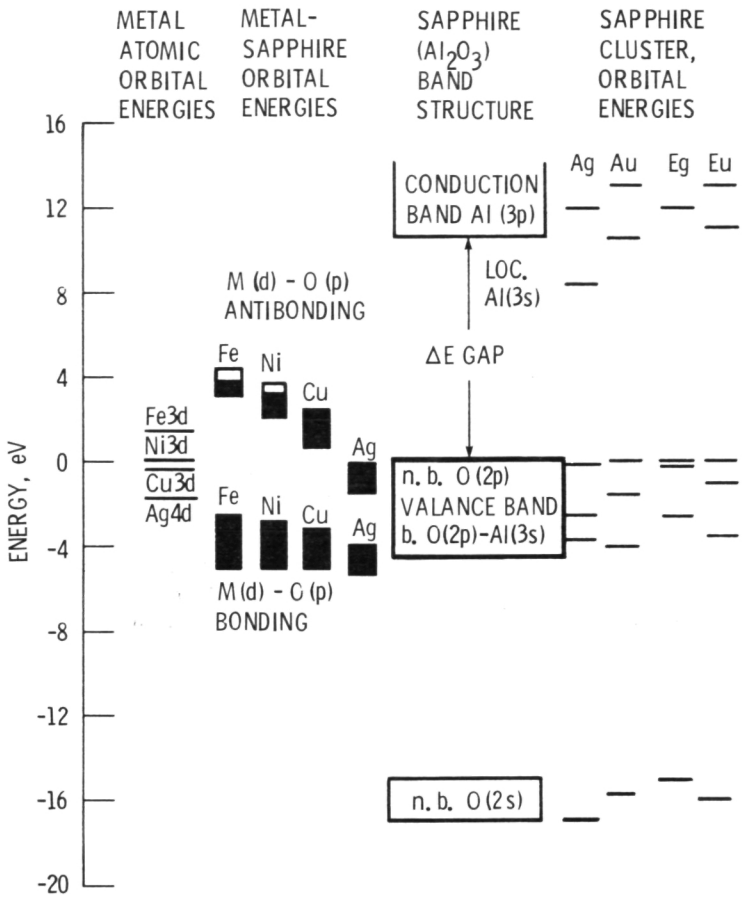

Figure 10. - Molecular-orbital energies, as determined by the self-consistent-field X-alpha scattered wave method, for clusters representing bulk sapphire and metal-sapphire interfaces.

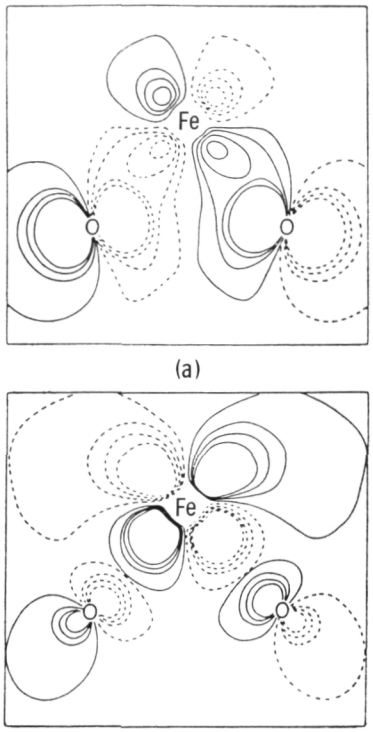

Figure 11. - Iron (d) and oxygen (p) molecular orbital wave-function contour maps for an iron atom supported on sapphire, plotted in the plane of the iron atom and two surface oxygen atoms, (a) occupied bonding, (b) unoccupied bonding. The solid and dashed contours represent the positive and negative phases of the wave function (ref. 10).

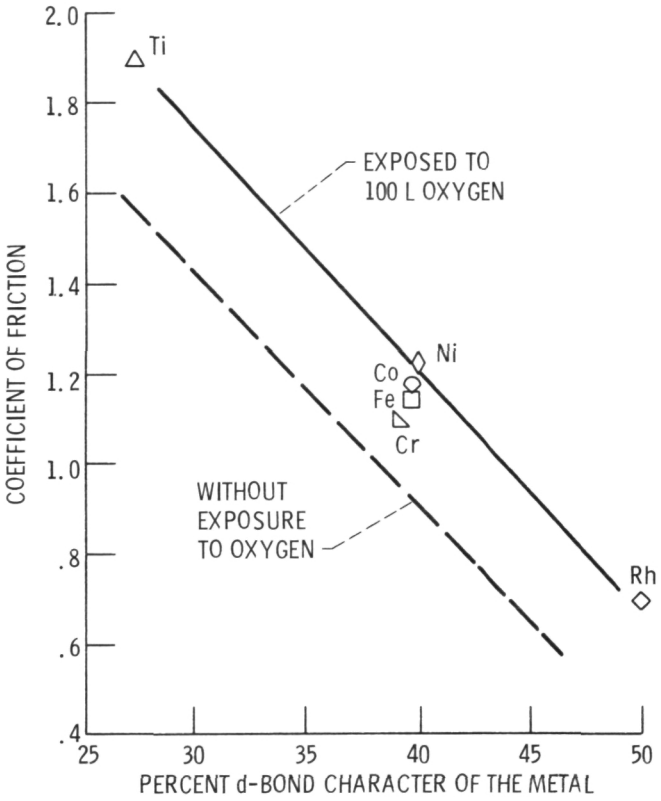

Figure 12. - Effect of adsorbed oxygen on friction for various metals in contact with the ferrites. Exposure, 1000 L in oxygen gas; sliding velocity, 3 mm/min; load, 0.05 to 0.2 N; vacuum, 3x10 nPa; room temperature.

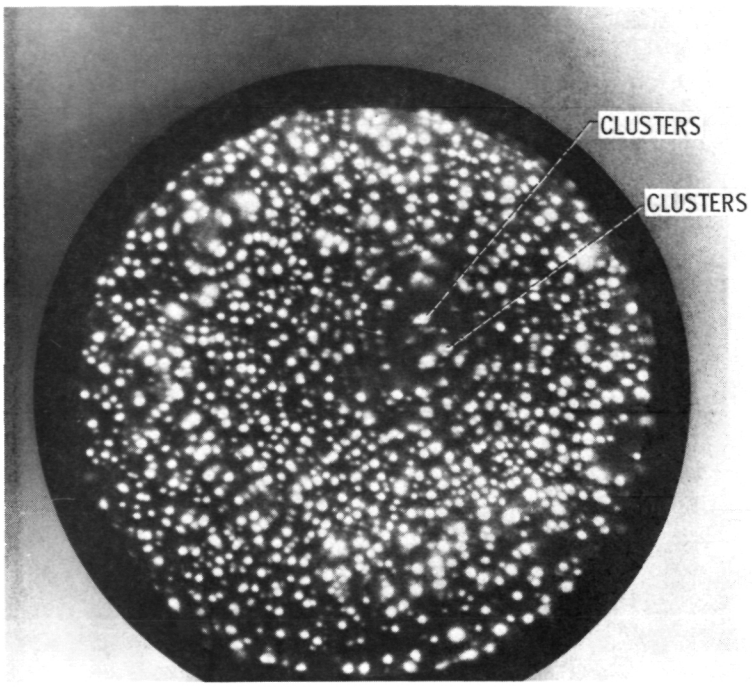

Figure 13. - Tungsten after gold contact at 13.0 kV with voltage raised to 14.5 kV for 30 sec; liquid-helium cooling.

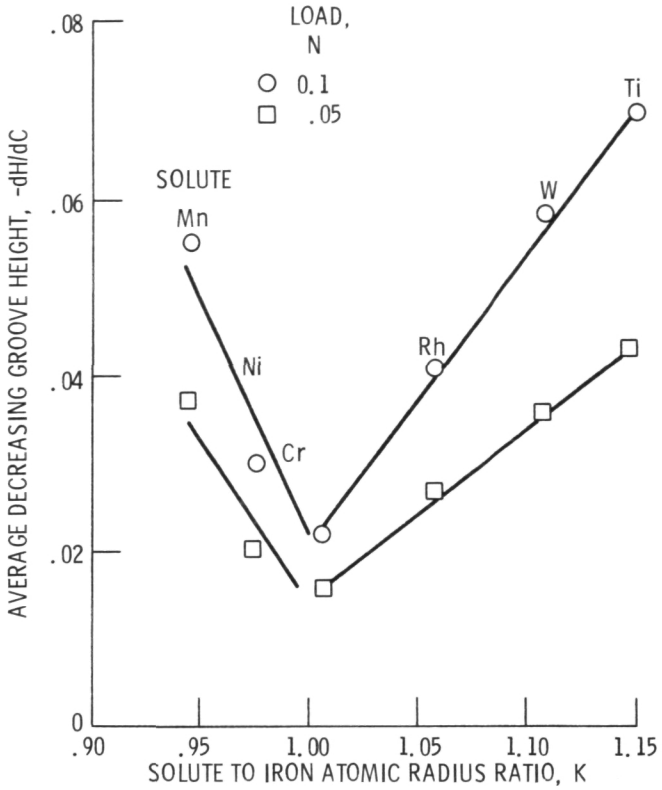

Figure 14. - Rates of change of groove height as function of solute to iron atomic radius ratio.

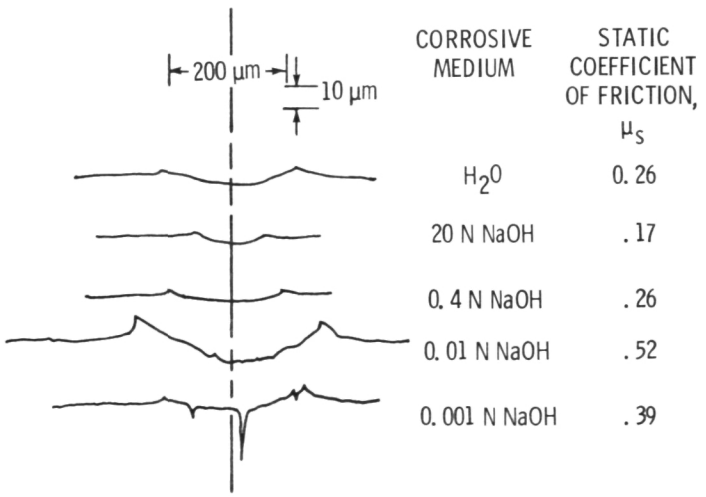

Figure 15. - Profilometer traverses across wear tracks generated by Al_2O_3 sphere sliding on iron flat in various media. (Wear tracks were made on iron flat.)

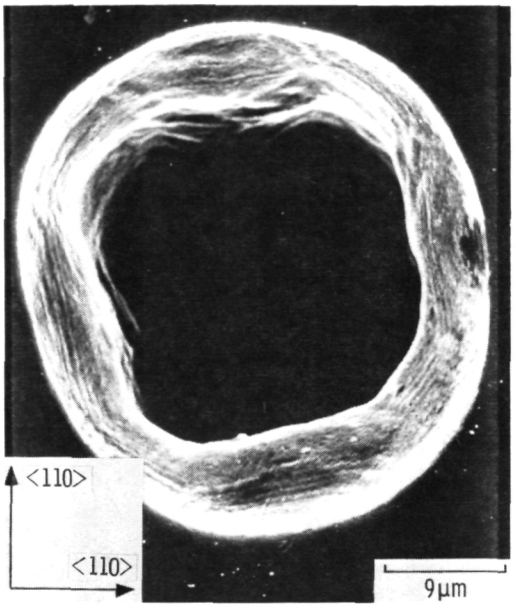

(a) t= 15 min, A typical pit on (001) face.

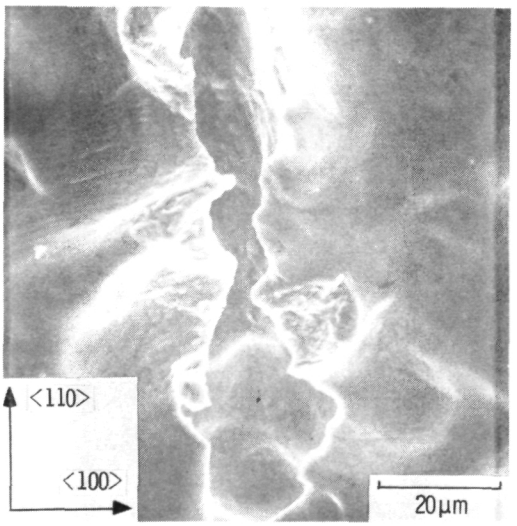

(b) t= 90 min, A typical pit on (110) face.

Figure 16. -Scanning electron micrographs of cavitation attack on α-brass single crystals.

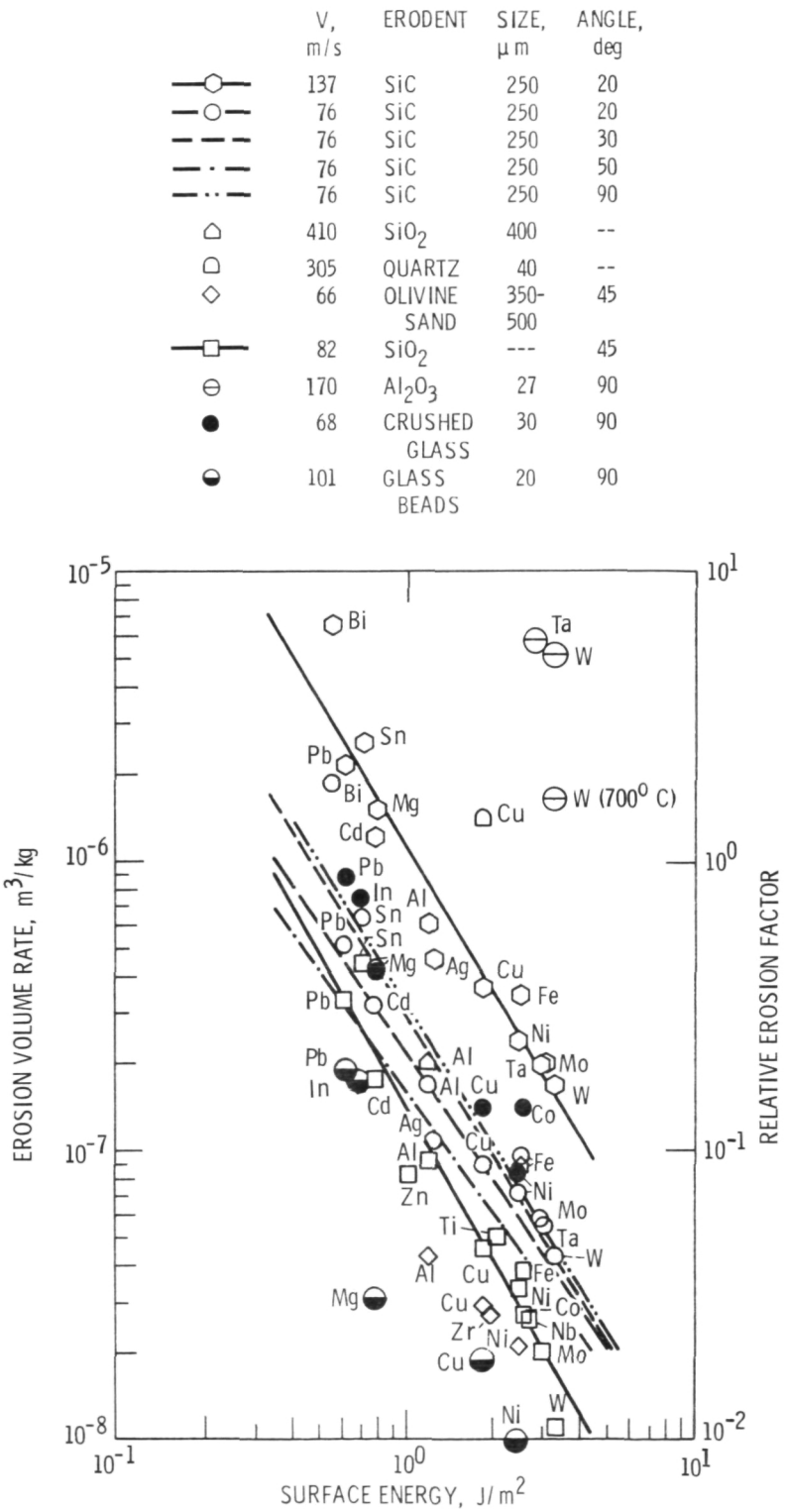

Figure 17. - Erosion rates of different metals as a function of surface energy.

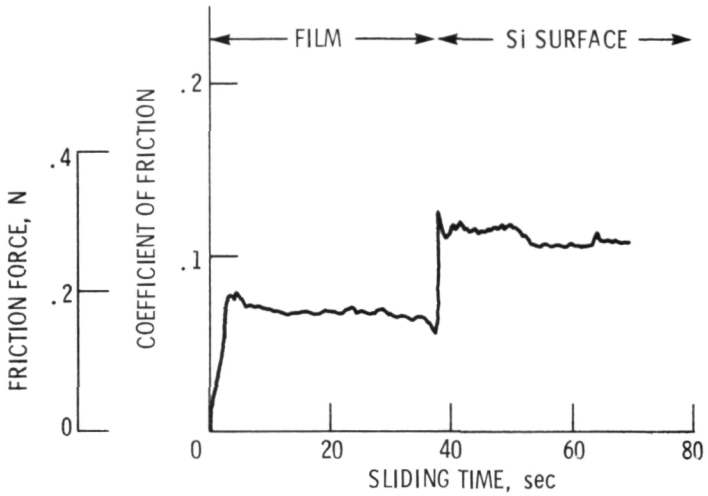

0.2 mm tip radius diamond rider, sliding velocity 10 mm/min, argon

Figure 18. - Coefficient of friction for diamond-like films on silicon.

ION BEAM DEPOSITED DIAMOND LIKE FILM WEAR

0.2 mm TIP RADIUS DIAMOND RIDER, SLIDING VELOCITY 10 mm/min, ARGON

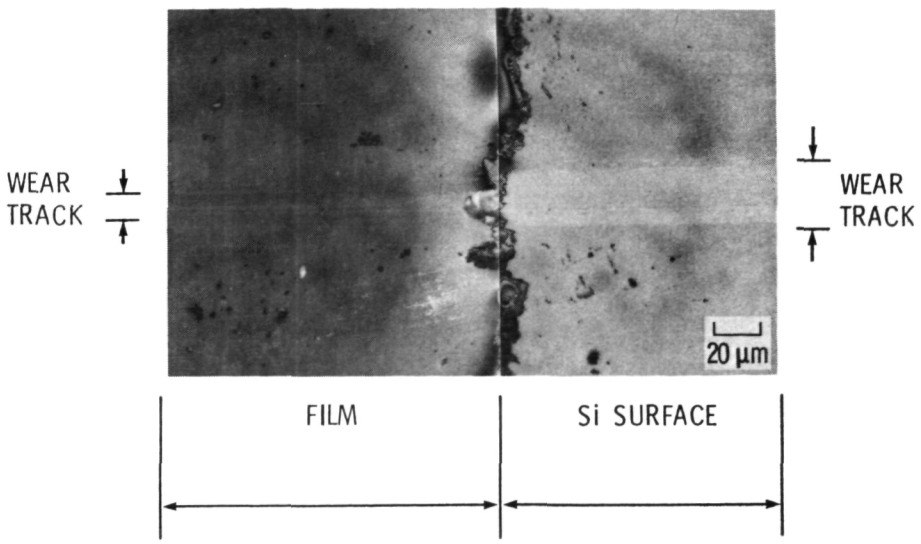

CS-85-1695

Figure 19.

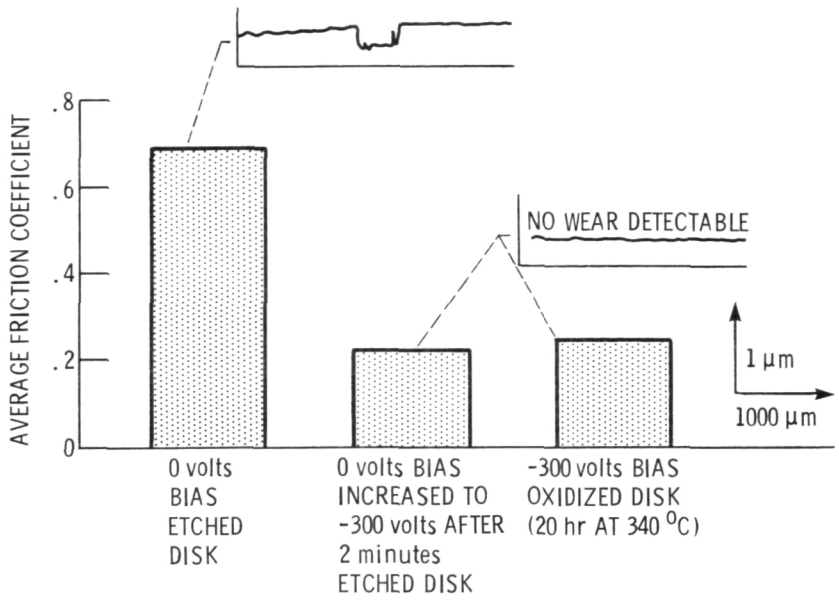

Figure 20. - Average friction coefficient and coating wear traces for RF sputtered Mo_2C on 440-C disk, 304 rider, 0.10 NT. Load, N_2 atmosphere.

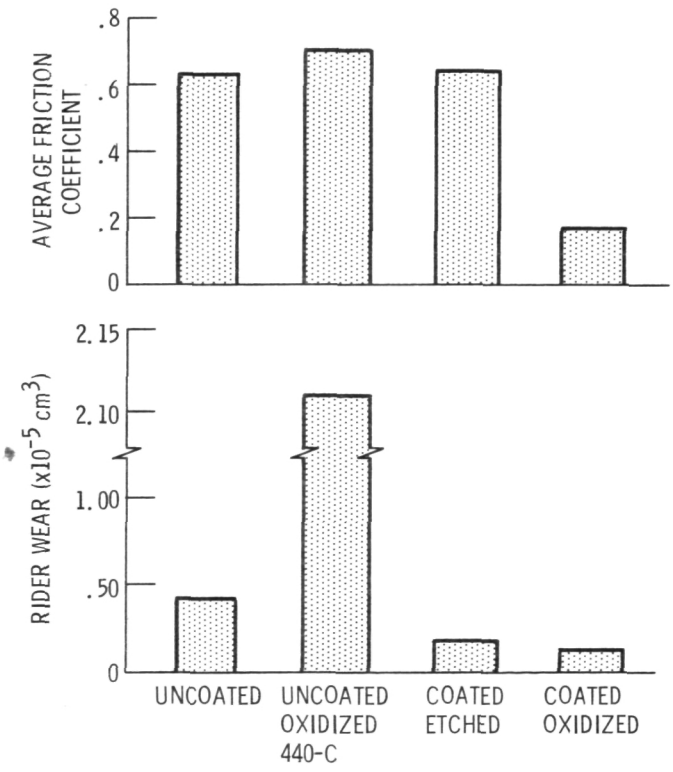

Figure 21. - Average friction coefficient and rider wear for 440-C disks either sputter etched (-1200 V for 15 min) or oxidized (20 hr at 340 °C). Coated disks are RF sputtered with TiB_2 (-300 V bias); load, 0.5 NT; N_2 atmosphere.

1. Report No.	2. Government Accession No.	3. Recipient's Catalog No.
NASA TM-87239		

4. Title and Subtitle	5. Report Date
Adhesion and Wear Resistance of Materials	
	6. Performing Organization Code: 506-43-01

7. Author(s)	8. Performing Organization Report No.
Donald H. Buckley	E-2914
	10. Work Unit No.

9. Performing Organization Name and Address	11. Contract or Grant No.
National Aeronautics and Space Administration Lewis Research Center Cleveland, Ohio 44135	
	13. Type of Report and Period Covered: Technical Memorandum

12. Sponsoring Agency Name and Address	14. Sponsoring Agency Code
National Aeronautics and Space Administration Washington, D.C. 20546	

15. Supplementary Notes

Prepared for the Hartstoffschichten zur Verschleißminderung sponsored by the Max-Planck-Institut für Metallforschung, Bad Honnef, Federal Republic of Germany, May 5-7, 1986. Invited paper.

16. Abstract

Recent studies, both analytical and experimental, into the nature of bonding at the interface between two solids in contact or a solid and deposited film have lent considerable insight into adhesive bonding. This has provided a better understanding of those properties important to the adhesive wear resistance of materials. Both analytical and experimental progress in the field are reviewed. For simple metal systems the adhesive bond forces are related to electronic wave function overlap where electronic structure and total energy are computed as a function of separation between the surfaces. With metals in contact with nonmetals such as oxide ceramics and diamond, molecular-orbital energy, and density of states, respectively can provide insight into adhesion and wear of the solid state contacts. Experimental results are presented which correlate adhesive forces measured between solids and the electronic surface structures. Orientation, surface reconstruction, surface segregation, adsorption are all shown to influence adhesive interfacial strength. Examples are presented for various classes of materials comprising the interface. The interrelationship between adhesion and the wear of the various materials as well as the life of coatings applied to substrates are discussed. Metallic systems addressed include simple metals and alloys and these materials in contact with themselves, both oxide and nonoxide ceramics, diamond, polymers, and inorganic coating compounds, such as diamond-like carbon. The role and mechanism of interfacial foreign species on adhesive bonding will also be presented.

17. Key Words (Suggested by Author(s))	18. Distribution Statement
Adhesion; Friction; Wear; Coatings	Unclassified - unlimited STAR Category 37

19. Security Classif. (of this report)	20. Security Classif. (of this page)	21. No. of pages	22. Price*
Unclassified	Unclassified		

*For sale by the National Technical Information Service, Springfield, Virginia 22161

National Aeronautics and
Space Administration

Lewis Research Center
Cleveland, Ohio 44135

NASA